THE UNIVERSITY OF BRITISH COLUMBIA

DEPARTMENT OF STATISTICS

TECHNICAL REPORT #271

Stochastic models for the effects of duration of load on lumber properties

BY

YONGLIANG ZHAI, NANCY HECKMAN,
CONROY LUM, CIPRIAN PIRVU,
LANG WU, JAMES V ZIDEK

October 2012

Stochastic models for the effects of duration of load on lumber properties

Yongliang Zhai[1], Nancy Heckman[1], Conroy Lum[2], Ciprian Pirvu[2], Lang Wu[1], Jim Zidek[1]
[1] The University of British Columbia
[2] FPInnovations, Vancouver, B.C.

Oct 2012

Abstract

The duration of load effect is a distinctive and important characteristic of wood strength. It refers to the fact that wood products can usually sustain higher loads for short time but lower loads for long time. Characterizing the duration of load effect and testing wood for specific properties of this effect are important in ensuring structural safety of wood construction.

This paper focuses on one well known damage accumulation model, the so–called US model because of both its importance and relative simplicity. We focus on methods for implementing that model and study their performance through simulation studies. We also demonstrate their use on a real dataset for illustration.

1 Introduction

This report presents statistical methods for fitting the so–called US Model that represents the impact of the duration of load effect on the allowable properties of dimension lumber. A thesis (Zhai 2012) and a companion paper Zhai et al. (2012) describe that effect in detail and review engineering approaches to the development of such models. We begin with a description of that effect for completeness.

Duration of load is associated with the creep-rupture behavior of wood products which may occur in the third phase of deformation under high constant loading. Under lower loads applied for long term, a wood product deforms or creeps and the rate of deformation is directly related to the magnitude and rate of loading, type of product and its properties, ambient environmental conditions, and the duration of loading. A product loaded within its elastic limits deforms but then returns to its initial state when the load is removed (i.e. it does not creep). When loaded beyond its elastic limits, a product does not return to its initial state because of the plastic/permanent deformations incurred (i.e. it creeps). The time-dependent deformation of a product under constant loading is called creep. Creep and duration of load effects of wood are of critical importance to timber engineering. To account for the duration of load behavior, design codes use adjustment factors recommended for sawn lumber and engineered wood products. The adjustment factors specified for wood products and connectors in the North American wood design standards are based on early damage accumulation models with parameters calibrated to experimental results for dimension lumber (Karacabeyli and Soltis, 1991).

Evaluation of load duration and creep requires extensive experimental testing, i.e., requires a large sample size subjected to long-term loading. In the early duration of load research program, load periods ranged from one to three years. More recent test programs involve shorter but still fairly substantial load periods. For example, a minimum 90-day constant load period in bending is required in the current standard ASTM D 6815 and a six-month period is required in the European standard for panel products.

As noted in Zhai et al. (2012), models for the effect are usually formulated in terms of the *accumulation of damage*. Accumulation of damage models have been proposed on a combination of incomplete understanding of the phenomena at the macroscopic level and experimental data (Yao, 1987). A piece of lumber is postulated to accumulate damage as a function of a load τ that may vary over time. The damage accumulated by time t is denoted by $\alpha(t)$ with,$\alpha(0) = 0$ and $\alpha(T) = 1$ by convention where T is the *breaking time* of the wood specimen. The damage α is a non-decreasing function of t. The amount of accumulated damage cannot be observed, but it may be inferred based on the observed breaking times.

All damage accumulation models are based on the following differential equation:

$$\frac{d\alpha(t)}{dt} = f(\alpha(t), \tau(t), \theta), \tag{1}$$

where f is a known function, $\tau(t)$ is the known load at time t, and θ is a vector of parameters, usually unknown. The short term strength τ_s is often included as an argument of f in equation (1), in the form of $\sigma(t) = \tau(t)/\tau_s$. However τ_s is defined in different ways. Gerhards and Link (1987) treat τ_s as a wood specimen dependent random parameter with an assumed distribution and do not define τ_s in terms of any breaking time or load pattern. Foschi and Yao (1986) also treat τ_s as a wood specimen dependent parameter, but define τ_s as the breaking load $\tau(T_s)$. in the ramp load test, when the loading rate k is set so that the mean breaking time is expected to be around one minute. Different definitions of τ_s lead to different damage accumulation models.

In the literature, the parameter vector θ is often treated as a constant vector, depending on the type of lumber but constant among wood specimens of the same type. However, this implies that all specimens of the same type, when subjected to the same load, have the same breaking time T, since, for a fixed θ and load, at most one value of T can satisfy $\alpha(T) = 1$. Clearly this is not realistic, as breaking times do vary from specimen–to–specimen. A perhaps more realistic approach is to treat the parameters θ as random effects, which vary from specimen–to–specimen. This approach was taken by Foschi and Yao (1982, 1986), as well as Gerhards and Link (1987).

Authors have proposed various parameter estimation methods based on breaking times obtained using experiments described in Section 2. However, the estimation of model parameters has been done in an ad hoc way leaving room for possible improvement. This paper explores inferential issues for the US Model due to its relative simplicity and importance, leaving other models to future work. In fact we consider the extension of that model obtained by adding random effects, one set for each randomly selected lumber specimen. Section 3 briefly describes that model for completeness, leaving a more detailed consideration to Zhai (2012) and Zhai et al. (21012a). Section 4 describes some parameter estimation methods for implementing it. A simulation study follows in Section 5 to compare the estimation methods. We then apply the methods to data obtained in the important experiments carried out by Foshi and Barrett (1982). Our conclusions are in Section 7.

2 Experimental methods

There are typically two types of duration of load tests: the ramp load test and the constant load test. In the ramp load test with rate k, the applied load is linear in t, that is $\tau(t) = kt$. The breaking time and load are T_s and $\tau(T_s) = kT_s$, respectively.

In the constant load test, the load first increases linearly at constant rate k until a predetermined time T_0, similar to the initial period of the ramp load test, and then the load remains constant during the rest of time That is

$$\tau(t) = \begin{cases} kt & \text{for } 0 \leq t \leq T_0, \\ kT_0 & \text{for } t > T_0. \end{cases}$$

The pre-determined load level kT_0 is denoted by τ_a, i.e., $\tau_a = kT_0$. The load level τ_a is usually set at a certain percentile of the empirical distribution of the short-term strength of the wood products tested during a ramp load test with load equal to kt, the same value of k as in the constant load test. The first part of the constant load test (i.e., $\tau(t) = kt$ when $0 \leq t \leq T_0$) is called the *ramp loading part of the constant load test* and the second part of the constant load test (i.e., $\tau(t) = \tau_a$ when $t > T_0$) is called the *constant loading part of the constant load test.*

3 The US Model

The US Model, also called the *exponential damage rate model (EDRM)*, which was proposed by Gerhards (1979), is given by

$$\frac{d\alpha(t)}{dt} = \exp\left\{-a + b\sigma(t)\right\}, \tag{2}$$

where a and b are model parameters. Here, $b > 0$. Some authors consider the parameters fixed while others consider the parameters random. The US Model has been discussed in Gerhard and Link (1987) as well as Foschi and Yao (1986). Although these represent the US Model in the same form in their papers, they actually discuss two different models based on their different definitions of the short term strength τ_s. Gerhards and Link treat the short term strength τ_s as a board dependent parameter and assume that τ_s follows a log-normal distribution with median τ_m. They do not define τ_s in terms of any breaking time or load pattern.

Foschi and Yao treat the US Model in a different way. They also consider the short term strength τ_s as a board dependent parameter, but they further define τ_s as the breaking load $\tau(T_s)$ of the ramp load test when the loading rate k is set so that the mean breaking time is expected to be around one minute. In both approaches, the breaking time is random since the short term strength τ_s is random. The Gerhards-Link and Foschi-Yao analyses have both similarities and differences in the ways they handle their analysis of the US Model which we now describe.

For the ramp load test, $\sigma(t) = kt/\tau_s$, we can integrate (2) to get $\alpha(t)$:

$$\alpha(t) = \int_0^t \exp\left(-a + bks/\tau_s\right) ds = \frac{\tau_s}{bk}\{\exp\left(-a + bkt/\tau_s\right) - \exp(-a)\}. \quad (3)$$

Since $\alpha(T_s) = 1$,

$$\frac{\tau_s}{bk}\{\exp\left(-a + bkT_s/\tau_s\right) - \exp(-a)\} = 1. \quad (4)$$

Gerhards and Link solve the above equation (4) for T_s in terms of a, b, k and τ_s. In contrast, Foschi and Yao solve the equation for T_s subject to $\tau_s = kT_s$, so Foschi and Yao solve solution for T_s does not contain τ_s as we will see in the sequel.

For the constant load test, if $T_s \leq T_0$ or equivalently, if $\alpha(T_0) \geq 1$, then the board breaks during ramp loading phase while if $T_s > T_0$, the breaking time T_c will depend on both the damage accumulated during ramp and constant loading phases. The former can be calculated from (3) as:

$$\alpha_0 = \alpha(T_0) \quad = \quad \frac{\tau_s}{bk}\{\exp\left(-a + b\tau_a/\tau_s\right) - \exp(-a)\}. \quad (5)$$

In the constant loading part of the test, $\tau(t) = \tau_a$, so we can integrate (2) from T_0 to find the damage accumulated and then find the total damage accumulated by time $t > T_0$:

$$\alpha(t) = \alpha_0 + \int_{T_0}^t \exp(-a + b\tau_a/\tau_s) ds = \alpha_0 + (t - T_0)\exp(-a + b\tau_a/\tau_s), \text{ for } t > T_0. \quad (6)$$

Setting $\alpha(T_c)$ in (6) equal to 1 and solving for T_c yields

$$T_c = T_0 + (1 - \alpha_0)/\exp(-a + b\tau_a/\tau_s) \quad (7)$$

if $T_c > T_0$.

Both Gerhards and Link as well as Foschi and Yao find T_c in this way. Gerhards and Link solve for T_c as in (7) in terms of a, b, k, T_0 and τ_s. Foschi and Yao solve for τ_s in terms of a and b, and substitute the result into (7), so Foschi and Yao's solution of T_c does not contain τ_s. The solutions appear below.

Gerhards and Link (1987) assume

$$\tau_s = \tau_m \exp(wR)$$

where τ_m is the median short term strength, w is a (unitless) scale parameter and R is a standard normal random effect.

Let $B = b/\tau_s = b/\{\tau_m \exp(wR)\}$. Then from (4):

$$T_s = \frac{\ln\{Bk\exp(a)+1\}}{Bk}, \tag{8}$$

with $T_s \neq \tau_s/k$. Substituting B for b/τ_s in (5), we can write α_0 as

$$\alpha_0 = \frac{1}{Bk}\{\exp(-a + B\tau_a) - \exp(-a)\}. \tag{9}$$

Substituting B for b/τ_s and substituting α_0 from (9) in (7), we can write T_c in the US Model as:

$$T_c = \begin{cases} \dfrac{\ln\{Bk\exp(a)+1\}}{Bk}, & \text{if } \dfrac{\ln\{Bk\exp(a)+1\}}{Bk} \leq T_0, \\ \\ T_0 - \dfrac{1}{Bk} + \exp(-B\tau_a)\left\{\dfrac{1}{Bk} + \exp(a)\right\}, & \text{if } \dfrac{\ln\{Bk\exp(a)+1\}}{Bk} > T_0. \end{cases} \tag{10}$$

Foschi and Yao (1986) define the short term strength of a board as its breaking strength in the ramp load test with the ramp loading rate k set so that the mean breaking time is around one minute. In other words, they solve for τ_s from $\tau_s = \tau(T_s) = kT_s$.

For the ramp load test, replacing τ_s by kT_s in (4), we get

$$T_s = \frac{\exp(a)b}{\exp(b)-1} \equiv Ab \tag{11}$$

where $A \equiv \exp(a)/\{\exp(b) - 1\}$. Since $\tau_s = kT_s$, (11) is equivalent to:

$$\tau_s = \frac{\exp(a)bk}{\exp(b) - 1} = Abk. \tag{12}$$

Substituting τ_s from (12) in (5) and (7), we obtain

$$T_c = \begin{cases} Ab, & \text{if } Ab \leq T_0, \\ T_0 + A\left\{\exp\left(b - T_0/A\right) - 1\right\}, & \text{if } Ab > T_0. \end{cases}$$

4 Estimation methods

This section presents several methods for estimating the parameters in the US Model for ramp and constant load tests. In the former, the loading rate k is set so that the mean breaking time is about one minute. In the constant load test, the constant load is set to be the p-th ($p < 0.5$) percentile of the breaking load in the ramp load test. We choose $p = 0.2$ as an illustration in this section. Zhai et al. (2012) extend US Model as given by Foschi and Yao (1986). Our version, the one considered in this report has

$$\frac{d\alpha(t)}{dt} = \lambda \exp\{-a + b\sigma(t)\}.$$

where $\lambda = 1$ hour^{-1}, a and b are unitless model parameters and $b > 0$. We first explore the maximum likelihood estimator (MLE). Other methods rely on approximations to the solutions of the failure times T_s and T_c. We consider both an approximate likelihood and a quantile method based on these approximate solutions. Finally we develop hybrid method that combines the approximate maximum likelihood and quantile methods.

With $A = \exp(a)/(\exp(b) - 1)$, the breaking time T_s in the ramp load test is given by:

$$\lambda T_s = Ab.$$

The breaking time T_c in the constant load test is given by:

$$\lambda T_c = \begin{cases} Ab, & \text{if } \ Ab \leq \lambda T_0, \\ \\ \lambda T_0 + A\left[\exp\left\{b - \lambda T_0/A\right\} - 1\right], & \text{if } Ab > \lambda T_0 \end{cases}$$

where T_0 is the loading time in the ramp loading part of the constant load test. For simplicity write T_s and T_c instead of λT_s and λT_c since $\lambda = 1$ hour^{-1}. The responses measured to yield the data are $\tilde{T}_s = (T_{s,1}, T_{s,2}, \cdots, T_{s,n_s})$ from the ramp load test, and $\tilde{T}_c = (T_{c,1}, T_{c,2}, \cdots, T_{c,n_c})$ from the constant load test.

We assume that a and b are two random variables following some distributions with means μ_a and μ_b, and variance σ_a^2 and σ_b^2 respectively. Let $\theta = (\mu_a, \mu_b, \sigma_a^2, \sigma_b^2)$ be the parameters to be estimated. We assume that a and b are independent. Define X and Y by

$$\begin{aligned} X &= Ab, &(13)\\ Y &= T_0 + A\left[\exp\{b - T_0/A\} - 1\right] \\ &= T_0 + \frac{X}{b}\left\{\exp\left(b - T_0\frac{b}{X}\right) - 1\right\}. &(14)\end{aligned}$$

Then T_s can be written as

$$T_s = X, \tag{15}$$

and T_c as

$$T_c = \begin{cases} X, & \text{if } X \le T_0, \\ Y, & \text{if } X > T_0. \end{cases} \tag{16}$$

4.1 The likelihood method

We consider data from three different experiments: a ramp load test; a constant load test with T_0 pre-determined independently of the constant load test; a ramp load test followed by a constant load test with T_0 depending on the ramp load test. Let f_{T_s} and f_{T_c} be the density functions of T_s and T_c respectively. These three experimental protocols then yield respectively the likelihoods:

$$L_s(\theta|\tilde{T}_s) = P(\tilde{T}_s|\theta) = \prod_{i=1}^{n_s} f_{T_s}(T_{s,i}|\theta). \tag{17}$$

$$L_c(\theta|\tilde{T}_c, T_0) = P(\tilde{T}_c|T_0, \theta) = \prod_{i=1}^{n_c} f_{T_c}(T_{c,i}|T_0, \theta). \tag{18}$$

$$
\begin{aligned}
L_b(\theta|\tilde{T}_s, \tilde{T}_c, T_0) &= P(\tilde{T}_s, \tilde{T}_c, T_0|\theta) \\
&= P(\tilde{T}_s|\theta)P(T_0|\tilde{T}_s, \theta)P(\tilde{T}_c|T_0, \tilde{T}_s, \theta) \\
&= P(\tilde{T}_s|\theta)P(\tilde{T}_c|T_0, \theta) \\
&= \prod_{i=1}^{n_s} f_{T_s}(T_{s,i}|\theta) \prod_{j=1}^{n_c} f_{T_c}(T_{c,j}|T_0, \theta). \qquad (19)
\end{aligned}
$$

The MLEs are found by maximizing the likelihood functions $L_s(\theta|\tilde{T}_s)$, $L_c(\theta|\tilde{T}_c, T_0)$ and $L_b(\theta|\tilde{T}_s, \tilde{T}_c, T_0)$. Because these functions are complicated, the quasi-Newton method is applied to calculate the maximum likelihood estimates.

The likelihood functions

In this section, we derive the likelihood functions $L_s(\theta|\tilde{T}_s)$, $L_c(\theta|\tilde{T}_c, T_0)$ and $L_b(\theta|\tilde{T}_s, \tilde{T}_c, T_0)$. To calculate the needed density functions of T_s and T_c, we need those of X and Y denoted f_X and f_Y respectively. The density function of T_s is

$$f_{T_s}(t|\theta) = f_X(t|\theta),$$

and the density function of T_c can be written as

$$f_{T_c}(t|\theta) = f_X(t|\theta)I(t \le T_0) + f_Y(t|\theta)I(t > T_0),$$

where I is the indicator function. To calculate the density function of X, we define the variable transformation as

$$\begin{cases} X = \dfrac{\exp(a)b}{\exp(b) - 1}, \\ V_1 = b. \end{cases}.$$

Then, a an b can be solved by

$$\begin{cases} a = \log \dfrac{X\{\exp(V_1) - 1\}}{V_1}, \\ b = V_1. \end{cases}$$

The Jacobian matrix J_s of this variable transformation is given by

$$J_s = \begin{pmatrix} \frac{\partial a}{\partial X} & \frac{\partial a}{\partial V_1} \\ \frac{\partial b}{\partial X} & \frac{\partial b}{\partial V_1} \end{pmatrix} = \begin{pmatrix} \frac{1}{X} & \frac{\exp(V_1)}{\exp(V_1)-1} - \frac{1}{V_1} \\ 0 & 1 \end{pmatrix}$$

The joint density function of X and V_1 is then

$$\begin{aligned} f_{X,V_1}(x,v) &= f_{a,b}\left(\log\frac{x\{\exp(v)-1\}}{v}, v\right)|J_s| \\ &= f_a\left(\log\frac{x\{\exp(v)-1\}}{v}\right) f_b(v)\frac{1}{|x|}. \end{aligned} \tag{20}$$

The marginal density function of X can be found by integrating the expression in (20):

$$f_X(x) = \int f_{X,V_1}(x,v)dv.$$

To calculate the density function of Y, we define the variable transformation as

$$\begin{cases} Y = T_0 + \dfrac{\exp(a)}{\exp(b)-1}\left[\exp\left\{b - T_0\dfrac{\exp(b)-1}{\exp(a)}\right\} - 1\right] \\ V_2 = \dfrac{\exp(a)}{\exp(b)-1}. \end{cases}$$

Then a and b can be found by solving

$$\begin{cases} a = \log\left\{(Y - T_0 + V_2)\exp\left(\dfrac{T_0}{V_2}\right) - V_2\right\} \\ b = \log\left(\dfrac{Y-T_0}{V_2} + 1\right) + \dfrac{T_0}{V_2}. \end{cases}$$

The Jacobian matrix J_c of this variable transformation is given by

$$J_c = \begin{pmatrix} \frac{\partial a}{\partial Y} & \frac{\partial a}{\partial V_2} \\ \frac{\partial b}{\partial Y} & \frac{\partial b}{\partial V_2} \end{pmatrix} = \begin{pmatrix} \frac{\exp(T_0/V_2)}{(Y-T_0+V_2)\exp(T_0/V_2)-V_2} & \frac{\exp(T_0/V_2)-(T_0/V_2)\exp(T_0/V_2)-1}{(Y-T_0+V_2)\exp(T_0/V_2)-V_2} \\ \frac{1}{Y-T_0+V_2} & \frac{-Y+T_0}{(Y-T_0)V_2+V_2^2} - \frac{T_0}{V_2^2} \end{pmatrix}$$

The joint density function of Y and V_2 is

$$\begin{aligned} f_{Y,V_2}(y,v) &= f_{a,b}\left(\log\left\{(y-T_0+v)\exp\left(\frac{T_0}{v}\right) - v\right\}, \log\left(\frac{y-T_0}{v}+1\right) + \frac{T_0}{v}\right)|J_c| \\ &= f_a\left(\log\left\{(y-T_0+v)\exp\left(\frac{T_0}{v}\right) - v\right\}\right) \\ &\quad \times f_b\left(\log\left(\frac{y-T_0}{v}+1\right) + \frac{T_0}{v}\right)|J_c| \end{aligned} \tag{21}$$

Finally the density function of Y can be found from (21):

$$f_Y(y) = \int f_{Y,V_2}(y, v)dv.$$

We can also calculate the density functions of the logarithm of the breaking times T_s and T_c and estimate the parameters in the logarithmic scale of the breaking times. These turn out to be simpler than those on the original scale for breaking times.

Optimization

We use the quasi-Newton method to optimize the likelihood functions. We choose a starting point for θ as $\theta^{(0)}$, and then update $\theta^{(0)}$ to $\theta^{(1)}$ by calculating the gradient of the likelihood functions with respect to θ at the value $\theta^{(0)}$. This recursive optimization routine is performed until convergence. We use *nlm* in R for optimization. For the choice of the starting point $\theta^{(0)}$, we use both the true values and random values in the simulation studies presented in the next section. For real data analysis, we do not have a good starting point $\theta^{(0)}$ and use random starting points in the analysis of data from Foschi and Barrett's experiments in Section 6.

Although the maximum likelihood estimates seem promising, it does not work well in practice because the integration limits are hard to determine. To solve this problem, we propose some approximations to the solutions for the breaking times in the US Model, in the next section.

4.2 Approximations

In this section, we discuss three approximations of the solutions for the breaking times in the US Model. The approximate solutions yield simple likelihoods. They are also used for the quantile method described in the next section.

We first approximate $\exp(b) - 1$ by $\exp(b)$ in the expressions of X and Y, yielding

$$
\begin{aligned}
X &= \frac{\exp(a)b}{\exp(b)-1} \\
&\overset{1}{\approx} \frac{\exp(a)b}{\exp(b)} \\
&= b\exp(a-b),
\end{aligned}
$$

$$
\begin{aligned}
Y &= T_0 + \frac{\exp(a)}{\exp(b)-1}\left\{\exp\left(b - T_0\frac{\exp(b)-1}{\exp(a)}\right) - 1\right\} \\
&\overset{1}{\approx} T_0 + \frac{\exp(a)}{\exp(b)}\left\{\exp\left(b - T_0\frac{\exp(b)}{\exp(a)}\right) - 1\right\},
\end{aligned}
$$

which we approximate further as

$$
\begin{aligned}
Y &\overset{2}{\approx} T_0 + \frac{\exp(a)}{\exp(b)}\exp\left\{b - T_0\frac{\exp(b)}{\exp(a)}\right\} \\
&= T_0 + \exp\{a - T_0\exp(b-a)\}.
\end{aligned}
$$

We then approximate the logarithm of X and the logarithm of $Y - T_0$ via Taylor series. For X, we expand $\log(b)$ about $\mu_b = E(b)$, and for $Y - T_0$, we expand $\exp(a-b)$ about $\mu_b - \mu_a = E(b) - E(a)$, yielding

$$
\begin{aligned}
\log(X) &\approx a - b + \log(b) \\
&\overset{3}{\approx} a - b + \log(\mu_b) + \frac{1}{\mu_b}(b - \mu_b), && (22) \\
\log(Y - T_0) &\approx a - T_0\exp(b-a) \\
&\overset{3}{\approx} a - T_0\exp(\mu_b - \mu_a)(b - a - \mu_b + \mu_a + 1). && (23)
\end{aligned}
$$

The approximations of the solutions for T_s and T_c can be written in terms of the approximations of X and Y.

For T_s, the first approximation yields

$$T_s \overset{1}{\approx} T_{s,approx1} \equiv b\exp(a-b), \tag{24}$$

and according to (22), the Taylor series expansion of T_s after the first approximation yields

$$\log(T_s) \overset{3}{\approx} \log(T_{s,approx3}) \equiv a - b + \log(\mu_b) + \frac{1}{\mu_b}(b - \mu_b). \tag{25}$$

For T_c, the first approximation yields

$$T_c \overset{1}{\approx} T_{c,approx1} \equiv \begin{cases} b\exp(a-b), & \text{if} \quad X \le \lambda T_0, \\ T_0 + \exp(a-b)\left[\exp\left\{b - T_0\exp(b-a)\right\} - 1\right], & \text{if} \quad X > \lambda T_0. \end{cases} \tag{26}$$

The second approximation yields

$$T_c \overset{2}{\approx} T_{c,approx2} \equiv \begin{cases} b\exp(a-b), & \text{if} \quad X \le \lambda T_0, \\ T_0 + \exp\{a - T_0\exp(b-a)\}, & \text{if} \quad X > \lambda T_0. \end{cases} \tag{27}$$

According to (22) and (23), the Taylor series expansions after the first two approximations yield

$$\begin{cases} \log(T_{c,approx3}) \equiv a - b + \log(\mu_b) + \dfrac{1}{\mu_b}(b - \mu_b), & \text{if} \quad X \le \lambda T_0, \\ \log(T_{c,approx3} - T_0) \equiv a - T_0\exp(\mu_b - \mu_a)(b - a - \mu_b + \mu_a + 1), & \text{if} \quad X > \lambda T_0. \end{cases} \tag{28}$$

We study the accuracy of our approximations by comparing T_s simulated from the original expressions (15) with T_s simulated from the approximations (24) and (25), and by comparing T_c simulated from the original expressions (16) with T_c simulated from the approximations (26), (27) and (28).

Approximation step 1

First approximate $\exp(b)-1$ by $\exp(b)$ in the solutions for the breaking times T_s and T_c. For large b, 1 is negligible compared to $\exp(b)$, so ee can write the ratio of X and the approximate X as

$$\frac{X}{X_{approx1}} = \frac{\exp(b)}{\exp(b)-1},$$

which is approximately 1 when b is large. Note that b must be positive and not unduly small to generate reasonable breaking times.

We conduct a simulation study to investigate the accuracy of the approximation step 1 when $\mu_b = 50$. The approximation error is negligible for both T_s and T_c when $\sigma_b = 0.4$ or $\sigma_b = 5$.

Approximation step 2

Step 2 approximates $\exp\{b - T_0 \exp(b-a)\} - 1$ by $\exp\{b - T_0 \exp(b-a)\}$ in the solution of T_c after the first approximation. To keep the mean breaking times in the ramp load test around one minute, μ_b should be bigger than μ_a and the difference should be between 6 and 8. Since T_0 is around 0.01, then $T_0 \exp(\mu_b - \mu_a) < 30$. We can show that $b - T_0 \exp(b-a) > 10$ for most pairs of the random variables (a, b). Thus 1 is negligible compared to $\exp\{b - T_0 \exp(b-a)\}$.

We have carried out simulation studies to investigate the accuracy of this approximation. In all simulation studies of this section, we assume that a and b are both Normal, $\mu_a = 42$ and $\mu_b = 50$, and $p = 0.2$ in the constant load test. We set $(\sigma_a, \sigma_b) = (0.4, 0.4)$, $(1, 5)$, $(5, 1)$ and $(5, 5)$. We simulate 1000 T_c's from the US Model with and without approximation steps 1 and 2, and then compare the differences of the T_c and the approximate T_c. Figure 1 contains plots of the approximation error versus the logarithm of the breaking time T_c. The logarithm of T_0 is indicated as the vertical line.

From Figure 1, we notice that the approximation step 2 is very accurate for most T_c's except for some values in the lower middle. We recall that approximation step 2 is only for the random variable Y, and T_c can be written in terms of X and Y as in (16). For $T_c \leq T_0$, we have that $T_c = X$ and the approximation step 2 is not used, so the only error is caused by the approximation step 1 and this error is small. For $T_c > T_0$, if we have that $T_c - T_0$ is close to 0, the approximation step 2 is not very accurate. However, the magnitude of the approximation error is still small. For $T_c > T_0$ and T_c much greater than T_0, the approximation is very accurate.

From Figure 1, we see that, the smaller σ_a and σ_b, the more inaccurate is the approximation when $T_c > T_0$ but close to T_0.

Thus the approximation step 2 is very accurate for most T_c's except for those in the starting stage of the constant loading part of the constant load test. However the magnitude of the difference caused by the approximation is still small.

Approximation step 3: linearization

This section discusses the linearization of the approximate random variables T_s and T_c on the logarithmic scale after the first two approximation steps. We can also linearize the random variable T_s and T_c without the first two

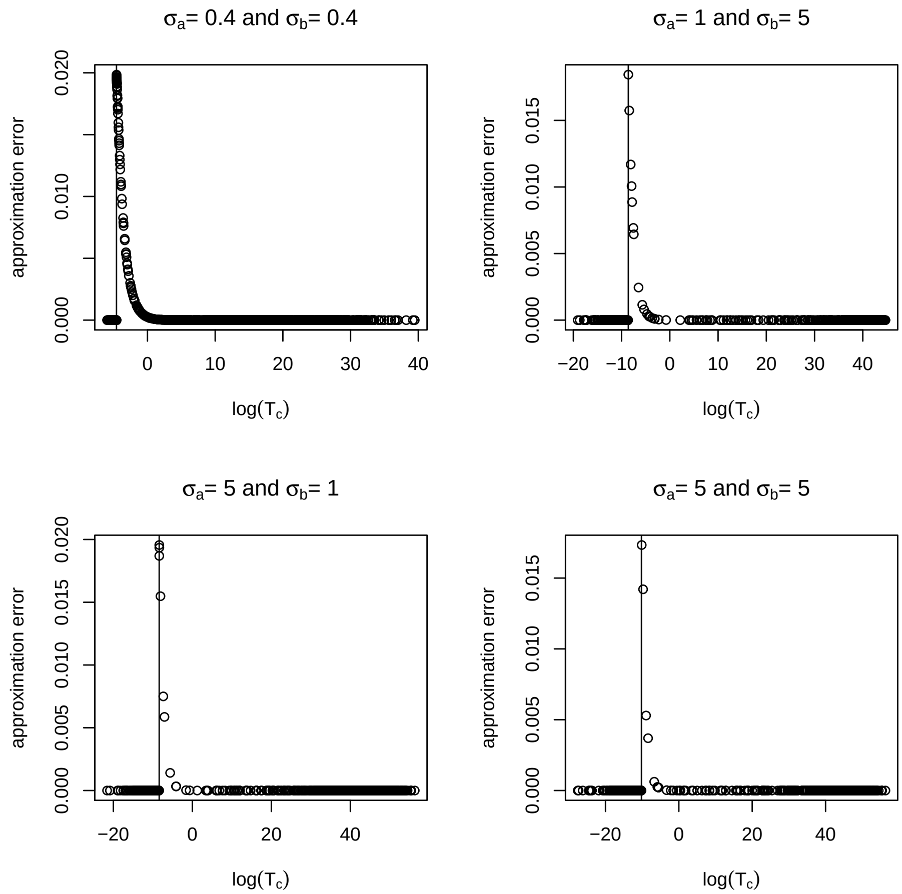

Figure 1: Plots of the approximation error versus the logarithm of the breaking time T_c when a and b are both Normal, $\mu_a = 42$ and $\mu_b = 50$, and $p = 0.2$ in the constant load test. The vertical line is $\log(T_0)$. The values for σ_a and σ_b are shown in the title. T_c's are the breaking times generated from the US Model without approximations and $T_{c,approx2}$'s are the approximated breaking times generated from the US Model with the approximation steps 1 and 2. The approximation error is the difference of $\log(T_{c,approx2})$ and $\log(T_c)$.

steps, but the results are complex and not very useful.

The linearization of the logarithm of the approximated random variable X after the approximation step 1 is given by the Taylor series about $\mu_b = E(b)$:

$$\begin{aligned} \log(X) &\approx a - b + \log(b) \\ &\approx a - b + \log(\mu_b) + \frac{1}{\mu_b}(b - \mu_b). \end{aligned} \tag{29}$$

Using the Lagrange form of the remainder of the Taylor series, the approximation error caused by the Taylor series is equal to

$$\frac{(\xi - \mu_b)^2}{2\mu_b^2},$$

where ξ is between b and μ_b. If we assume that b is Normal, by the empirical rule, it can be shown that

$$\begin{aligned} & P\left\{\frac{(\xi - \mu_b)^2}{2\mu_b^2} > \frac{9\sigma_b^2}{2\mu_b^2}\right\} \\ \leq\ & P\left\{\frac{(\xi - \mu_b)^2}{2\mu_b^2} > \frac{9\sigma_b^2}{2\mu_b^2}\right\} \\ =\ & P\left\{(\xi - \mu_b)^2 > 9\sigma_b^2\right\} \\ \leq\ & P(|b - \mu_b| > 3\sigma_b) \\ <\ & 0.01. \end{aligned}$$

The last inequality is from the empirical rule (or so-called three-σ rule). We choose the value $9\sigma_b^2/2\mu_b^2$ to use the empirical rule. The above result means when σ_b is small and μ_b is large, the approximation error caused by linearization is negligible with a probability close to 1.

We can write the approximation error caused by the Taylor series expansion of the logarithm of X as

$$\log(X) - \log(X_{approx}) = \log\left(\frac{b}{\mu_b}\right) + \frac{1}{\mu_b}(b - \mu_b), \tag{30}$$

which also shows that the linearization is more accurate when b is closer to μ_b.

The linearization of the logarithm of the random variable $Y - T_0$ after the approximation steps 1 and 2 is given by the Taylor series expansion of

$\exp(b-a)$ about $\mu_b - \mu_a$:

$$\begin{aligned} \log(Y - T_0) &\approx a - T_0 \exp(b-a) \\ &\approx a - T_0 \exp(\mu_b - \mu_a)(b - a - \mu_b + \mu_a + 1). \end{aligned} \tag{31}$$

Using the Lagrange form of the remainder of the Taylor series, the approximation error caused by the Taylor series expansion is equal to

$$\frac{1}{2} T_0 \exp(\mu_b - \mu_a)\{\xi - (\mu_b - \mu_a)\}^2,$$

where ξ is between $b-a$ and $\mu_b - \mu_a$. However, unlike the linearization of X, the approximation error caused by the linearization of $Y - T_0$ is only negligible when $b - a$ is very close to $\mu_b - \mu_a$.

We performed a simulation study to investigate the accuracy of the linearization and the approximate breaking times T_s's and T_c's are calculated after all three approximations. Figure 2 plots of the approximation error versus the logarithm of the breaking time T_s. Figure 3 plots of the approximation error versus the logarithm of the breaking time T_c.

Figure 2 suggests the Taylor series expansion for T_s is reasonably accurate. In all panels, the magnitude of the approximation errors is relatively small compared to the magnitude of T_s for all panels. In the upper left panel of Figure 2, the magnitude of the approximation errors is much smaller than in the other panels, which means the Taylor series expansion is more accurate when σ_b is small, as shown in (30). However, in the other three panels, the magnitude of the approximation errors is still relatively small compared to the magnitude of T_s's for most values. In the upper right panel of Figure 2, we see a pattern of the change of the approximations errors when T_s increases, which does not appear in the other three panels.

From Figure 3, the Taylor series expansion for T_c is accurate for the values which are close to the median of T_c (indicated by the vertical line). As we can infer from (31), the Taylor series expansion of a random viable with the exponential form is only accurate for the values very close to the fixed point chosen for the Taylor's expansion. From the upper left panel of Figure 3, the approximation errors increases slowly when T_c departs from the median. However, the approximation errors increases rapidly when T_c departs from the median in the other three panels.

In conclusion, the linearization works acceptably well for T_s's, but only works well for those T_c's close to the median of T_c.

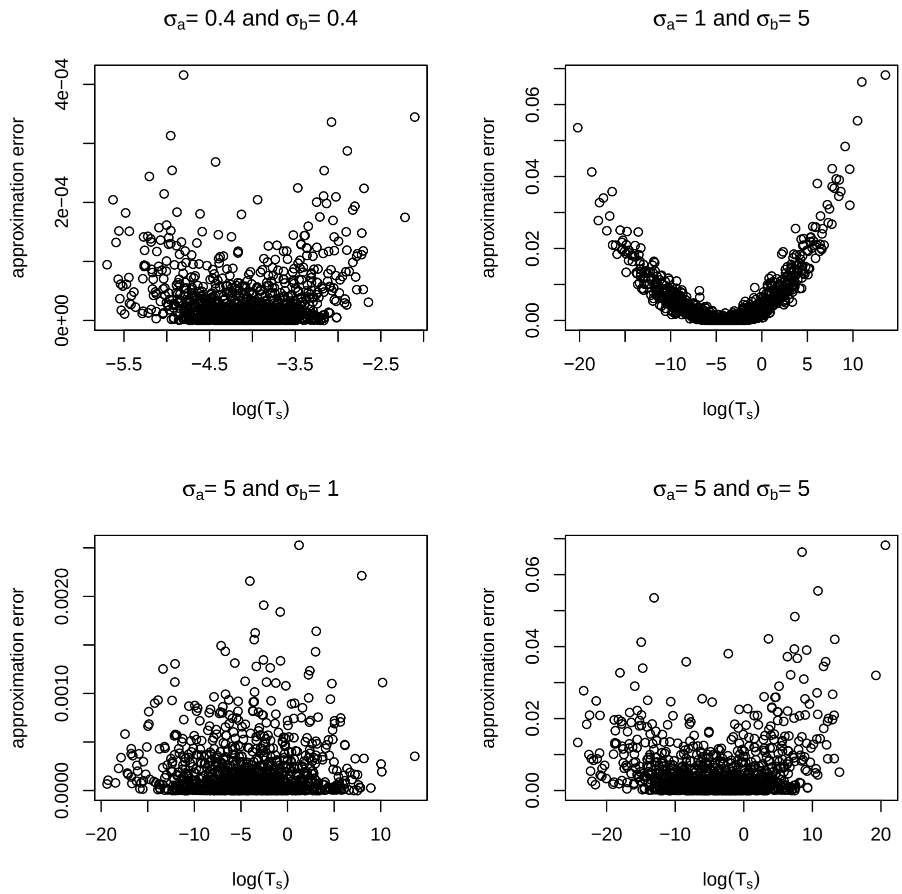

Figure 2: Plots of the approximation error versus the logarithm of the breaking time T_s when a and b are both Normal, $\mu_a = 42$ and $\mu_b = 50$. The values for σ_a and σ_b are shown in the title. T_s's are the breaking times generated from the US Model without approximations and $T_{s,approx3}$'s are the approximated breaking times generated from the US Model with the approximation steps 1, 2 and 3. The approximation error is the difference of $\log(T_{s,approx3})$ and $\log(T_s)$.

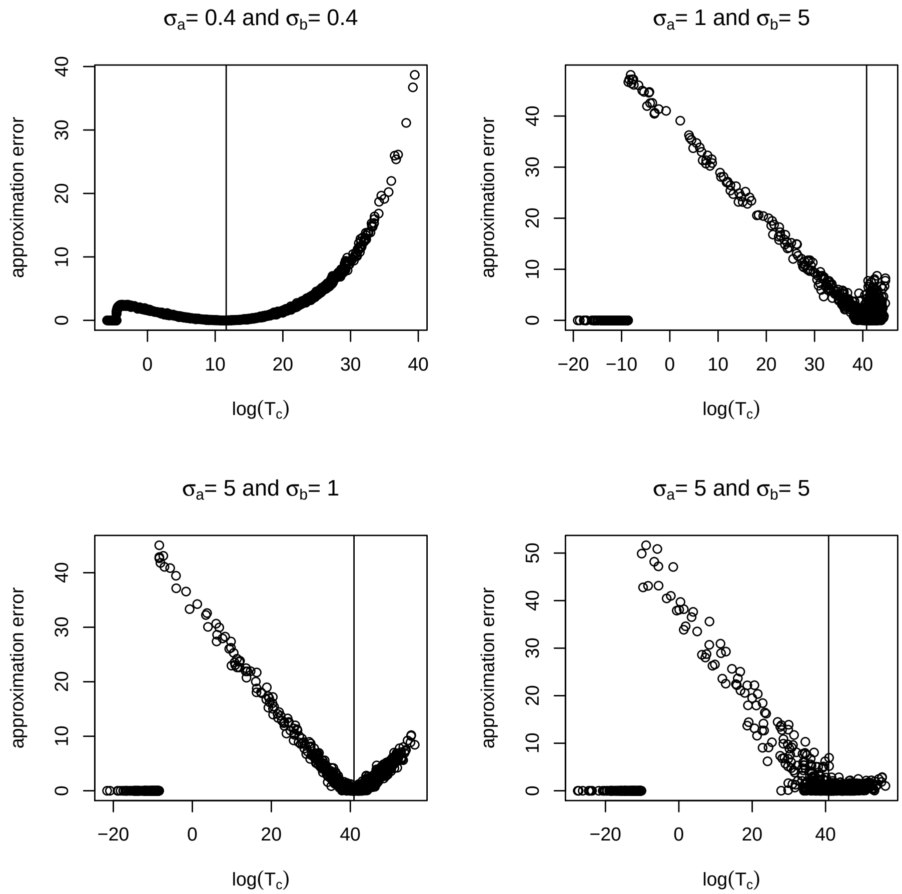

Figure 3: Plots of the approximation error versus the logarithm of the breaking time T_c when a and b are both Normal, $\mu_a = 42$ and $\mu_b = 50$, and $p = 0.2$ in the constant load test. The values for σ_a and σ_b are shown in the title. T_c's are the breaking times generated from the US Model without approximations and $T_{c,approx3}$'s are the approximated breaking times generated from the US Model with the approximation steps 1, 2 and 3.The vertical line denotes the logarithm of the median of the breaking times T_c's. The approximation error is the difference of $\log(T_{c,approx3})$ and $\log(T_c)$.

Approximate likelihood functions

The likelihood functions involving the original solutions T_s and T_c of the US Model were seen above to be very complex which makes the integration and optimization processes involved impractical. In contrast, the likelihood functions for the approximate solutions for T_s and T_c are easier to calculate. Those results show the approximations from steps 1 and 2 to be very accurate for most values of T_s and T_c. So to calculate the approximate likelihood functions, we use the approximate solution for T_s in (25) and the approximate solution for T_c in (28) obtained following steps 1 and 2. Simulation studies to evaluate the performance of these approximate maximum likelihood estimates are discussed in Section 5.

4.3 Quantile method

For the distribution of breaking times, this section presents the quantile method for parameter estimation based on moment and quantile estimates. It is based on our approximations to T_s and T_c. We discuss the quantile method under the constraint that b is positive. In the revised US Model, b is defined as positive, formally negating the assumption that b has the normal distribution. However if the standard deviation σ_b is small relative to the expected value of b, the probability of b is non-positive is negligible.

From (29) and (31), $\log(X)$ and $\log(Y - T_0)$ can be written as linear combinations of the random variables a and b, i.e.,

$$\begin{aligned}\log(X) &\approx a - (1 - 1/\mu_b)b + \log(\mu_b) - 1,\\ \log(Y - T_0) &\approx a + c_0 a - c_0 b - c_0(\mu_a - \mu_b + 1),\end{aligned}$$

where $c_0 = T_0 \exp(\mu_b - \mu_a)$.

If a and b are independent, then

$$\begin{aligned}E\{\log(X)\} = \mu_a - \mu_b + \log(\mu_b), &\quad var\{\log(X)\} = \sigma_a^2 + (1 - 1/\mu_b)^2\sigma_b^2,\\ E\{\log(Y - T_0)\} = \mu_a - c_0, &\quad var\{\log(Y - T_0)\} = (1 + c_0)^2\sigma_a^2 + c_0^2\sigma_b^2.\end{aligned}$$

We denote the means of $\log(X)$ and $\log(Y - T_0)$ as μ_X and μ_Y respectively, and the variances of $\log(X)$ and $\log(Y - T_0)$ as σ_X^2 and σ_Y^2 respectively. We can estimate μ_a and μ_b from the estimates of μ_X and μ_Y. The equations

$$\begin{cases}\mu_X = \mu_a - \mu_b + \log(\mu_b),\\ \mu_Y = \mu_a - T_0 \exp(\mu_b - \mu_a),\end{cases}$$

$$(32)$$

yield

$$\mu_X - \mu_Y + \mu_b - \log(\mu_b) - T_0\mu_b \exp(-\mu_X) = 0. \quad (33)$$

We can numerically solve for μ_b from (33) given the estimates of μ_X and μ_Y, and then solve for μ_a from (32).

We can estimate σ_a^2 and σ_b^2 from the estimates of σ_X^2 and σ_Y^2. The equations

$$\begin{cases} \sigma_X^2 = \sigma_a^2 + (1 - 1/\mu_b)^2\sigma_b^2, \\ \sigma_Y^2 = (1 + c_0)^2\sigma_a^2 + c_0^2\sigma_b^2, \end{cases} \quad (34)$$

yield

$$\begin{cases} \sigma_a^2 = \sigma_X^2 - (1 - 1/\mu_b)^2[(1 + c_0)^2\sigma_X^2 - \sigma_Y^2]/\{(1 + c_0)^2(1 - 1/\mu_b)^2 - c_0^2\}, \\ \sigma_b^2 = \{(1 + c_0)^2\sigma_X^2 - \sigma_Y^2\}/\{(1 + c_0)^2(1 - 1/\mu_b)^2 - c_0^2\}. \end{cases} \quad (35)$$

We can solve for σ_a^2 and σ_b^2 in (35) given μ_a, μ_b, σ_X^2 and σ_Y^2.

To estimate μ_X, μ_Y, unlike σ_X and σ_Y, we do not need to require that a and b be normally distributed The estimation errors of the quantile method consist of the random error and the approximation error. The random error can be reduced by increasing the sample size, and the effect of the approximation error can be reduced by choosing reasonable quantiles.

4.4 Estimates of the means

Let m_X, m_Y, m_{T_s} and m_{T_c} be the medians of the distributions of X, Y, T_s and T_c respectively. From the ramp load test, we observe $T_s = X$, so we can simply estimate μ_X by the sample mean of the logarithm of the measured T_s's. We can also estimate μ_X by the median of the logarithm of the measured T_s's if $\log(T_s)$ is symmetrically distributed. From the constant load test, we observe the $\{T_c\}$, which are equal to X or Y according as $X \leq T_0$ or $X > T_0$ by (16) where T_0 is set to be the p–percentile ($p < 0.5$) of the $\{T_s\}$ from the ramp load test. However, we cannot estimate μ_Y by the sample mean of the logarithm of the observed $T_c - T_0$ since

$$E\{\log(T_c - T_0)\} \neq \mu_Y. \quad (36)$$

Instead, when $\log(Y - T_0)$ is symmetrically distributed, we can estimate μ_Y by the logarithm of the median of the $T_c - T_0$'s provided we can show that

$$m_{T_c} = m_Y = \exp(\mu_Y) + T_0. \tag{37}$$

Theorem 1. *The median of T_c equals the median of Y when b is positive and $p < 0.5$.*

Proof. To show that $m_{T_c} = m_Y$, we calculate $P(T_c \geq m_Y)$:

$$\begin{aligned} P(T_c \geq m_Y) &= P(T_c \geq m_Y, X \leq T_0) + P(T_c \geq m_Y, X > T_0) \\ &= P(X \geq m_Y, X \leq T_0) + P(Y \geq m_Y, X > T_0) \\ &= P(m_Y \leq X \leq T_0) + P(Y \geq m_Y)P(X > T_0 | Y \geq m_Y) \\ &= P(m_Y \leq X \leq T_0) + 0.5P(X > T_0 | Y \geq m_Y). \end{aligned} \tag{38}$$

Notice that T_0 is the p–percentile ($p < 0.5$) of X, so the median of X, which is the 50-th percentile of X, is larger than T_0, i.e., $T_0 < m_X$. Notice also that if $X > T_0$, then

$$Y > X. \tag{39}$$

because according to (14),

$$\begin{aligned} Y &= T_0 + \frac{X}{b}\left\{\exp\left(b - b\frac{T_0}{X}\right) - 1\right\} \\ &> T_0 + \frac{X}{b}\left\{1 + b - b\frac{T_0}{X} - 1\right\} \\ &= T_0 + X - T_0 \\ &= X. \end{aligned}$$

As a result, the median of X is smaller than the median of Y, i.e.,

$$T_0 < m_X < m_Y, \tag{40}$$

which yields

$$P(m_Y \leq X \leq T_0) = 0$$

in the first part of equation (38).

Next we observe that the definition of Y in (14) yields

$$X > T_0 \Leftrightarrow Y > T_0. \tag{41}$$

The reason is that, $b > 0$ and according to (14),

$$\begin{aligned} X > T_0 &\Leftrightarrow b > b\frac{T_0}{X} \\ &\Leftrightarrow \exp\left(b - b\frac{T_0}{X}\right) > 1 \\ &\Leftrightarrow \frac{X}{b}\left\{\exp\left(b - b\frac{T_0}{X}\right) - 1\right\} > 0 \\ &\Leftrightarrow T_0 + \frac{X}{b}\left\{\exp\left(b - b\frac{T_0}{X}\right) - 1\right\} > T_0 \\ &\Leftrightarrow Y > T_0. \end{aligned}$$

Therefore the second part of equation (38) can be calculated as

$$0.5P(X > T_0 | Y \geq m_Y) = 0.5P(Y > T_0 | Y \geq m_Y) = 0.5 \times 1 = 0.5, \quad (42)$$

since $m_Y > T_0$ as shown in (40).

To sum up, we have shown that under the constraint $b > 0$,

$$P(T_c \geq m_Y) = 0.5. \quad (43)$$

□

As a corollary of Theorem 1, μ_Y can be estimated by the logarithm of the median of T_c minus T_0 when $\log(Y - T_0)$ is symmetrically distributed.

The above proof is not true when b is assumed to be normally distributed since b can then be negative. However if the standard deviation σ_b is small, the equation (43) can be approximated as

$$P(T_c \geq m_Y) \approx 0.5. \quad (44)$$

Under the assumption that b is normally distributed, we demonstrate the plausibility of (44) by simulation plots. We first simulate 1000 X's to calculate T_0. Then we simulate another 1000 pairs of (a, b)'s and calculate the X's, Y's and T_c's for each pair. We paint all the simulated points grey, and then paint those points which satisfy $T_c > m_Y$ black. The plots are shown in Figure 4.

From Figure 4, we notice that the proportion of the points which satisfy $T_c \geq m_Y$ is around 0.5, although the border line is not of the same shape for different values of the standard deviations. We also confirm this by counting the number of points which satisfy that $T_c \geq m_Y$, which is 500 for every plot.

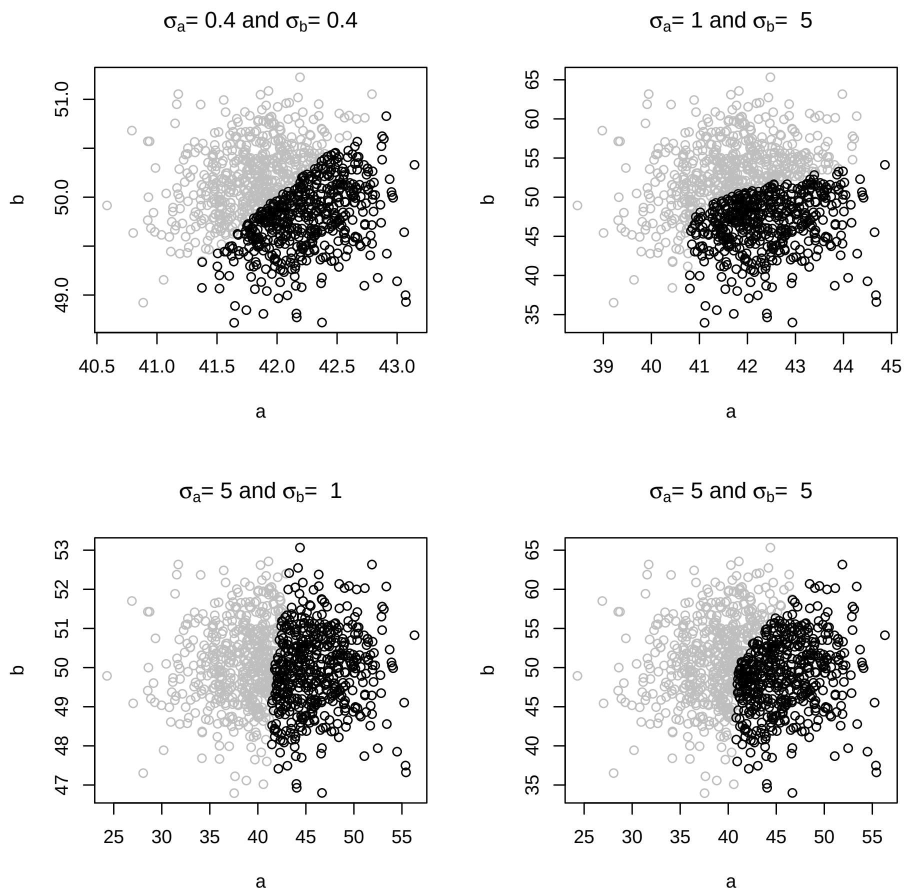

Figure 4: Plots for illustrating the quantile method when a and b are both Normal, $\mu_a = 42$ and $\mu_b = 50$, and $p = 0.2$ in the constant load test. The values for σ_a and σ_b are shown in the title. We paint all the simulated points grey, and then paint those points which satisfy $T_c > m_Y$ black. These plots support our claim in equation (44).

Estimates of the variances

If a and b are both assumed to be normally distributed, then $\log(X)$ and $\log(Y - T_0)$ are both approximately Normal, i.e.,

$$\log(X) \sim N(\mu_X, \sigma_X^2), \tag{45}$$

where $\mu_X = \mu_a - \mu_b + \log(\mu_b)$ and $\sigma_X^2 = \sigma_a^2 + (1 - 1/\mu_b)^2\sigma_b^2$, and

$$\log(Y - T_0) \sim N(\mu_Y, \sigma_Y^2), \tag{46}$$

where $c_0 = T_0 \exp(\mu_b - \mu_a)$, $\mu_Y = \mu_a - c_0$ and $\sigma_Y^2 = (1 + c_0)^2\sigma_a^2 + c_0^2\sigma_b^2$.

For the ramp load test, we can simply estimate σ_X^2 by the sample variance of the logarithm of the T_s's and σ_X^2 by the quantiles of the logarithm of the $\{T_s\}$. Let $t_{1,s}$ and $t_{2,s}$ be the $p_{1,s}^{\text{th}}$ quantile and the $p_{2,s}^{\text{th}}$ quantile of the logarithm of the $\{T_s\}$. Because $\log(T_s)$'s distribution is approximately normal after the linearization under the normal assumptions on a and b, the difference of $t_{2,s} - t_{1,s}$ is linked to σ_X, i.e.,

$$t_{2,s} - t_{1,s} = c_s\sigma_X$$

where c_s is a constant depending on $p_{1,s}$ and $p_{2,s}$. For example, if we choose $p_{1,s} = 0.1587$ and $p_{2,s} = 0.8413$, then $t_{2,s} - t_{1,s} \approx 2\sigma_X$ according to the empirical rule.

For the constant load test, we cannot estimate σ_Y^2 by the variance of the logarithm of the $\{(T_c - T_0)\}$ since not all of the T_c's are defined as Y's. However, we can still use the quantile estimates. Let $t_{1,c}$ and $t_{2,c}$ be the $p_{1,c}$ quantile and the $p_{2,c}$ quantile of the logarithmic of the $T_c - T_0$'s. Let $q_{1,Y}$ and $q_{2,Y}$ be the $p_{1,c}$ quantile and the $p_{2,c}$ quantile of the logarithm of $Y - T_0$'s. If we can show that $t_{1,c} = q_{1,Y}$ and $t_{2,c} = q_{2,Y}$, then

$$t_{2,c} - t_{1,c} = q_{2,Y} - q_{1,Y} = c_c\sigma_Y \tag{47}$$

where c_c is a constant depending on $p_{1,c}$ and $p_{2,c}$.

We can prove that $t_{1,c} = q_{1,Y}$ and $t_{2,c} = q_{2,Y}$ using the same method as in the proof above for the median estimates under the conditions that $b > 0$, $p_{1,c} > p$ and $p_{2,c} > p$. Since the logarithmic transformation and the shift transformation do not affect the quantiles, we only need to show that the $p_{1,c}^{\text{th}}$ (or $p_{2,c}^{\text{th}}$) quantile of T_c equals the $p_{1,c}^{\text{th}}$ (or $p_{2,c}^{\text{th}}$) quantile of Y when b is positive and $p_{1,c} > p$ (or $p_{2,c} > p$).

Theorem 2. *The $p_{1,c}$-th (or $p_{2,c}$-th) quantile of T_c equals the $p_{1,c}$-th (or $p_{2,c}$-th) quantile of Y, when b is positive and $p_{1,c} > p$ (or $p_{2,c} > p$).*

The proof of the above Theorem 2 is similar to the proof of Theorem 1. We need only change m_Y in the proof of Theorem 1 to $q_{1,Y}$ (or $q_{2,Y}$), and change 0.5 in the proof of Theorem 1 to $p_{1,c}$ (or $p_{2,c}$) to get a proof of Theorem 2. Note that in the above proof, we require $p_{1,c} > p$ and $p_{2,c} > p$. Therefore, we cannot choose $p_{1,c}$ too small. For example, if $p = 0.2$, we can choose $0.3 \leq p_{1,c} \leq 0.5$ and $p_{2,c}$ larger than 0.5.

Approximation errors

As noted above the linearization is not accurate for all T_c's, and the farther T_c is from the median, the less accurate is the linearization (see Figure 3). Therefore, we should choose $p_{1,c}$ and $p_{2,c}$ close to 0.5 to reduce the approximation errors.

Choosing reasonable values for $p_{1,s}$, $p_{2,s}$, $p_{1,c}$ and $p_{2,c}$ seems quite challenging. In the simulation studies, we chose $p_{1,s} = 0.2$, $p_{2,s} = 0.8$, $p_{1,c} = 0.45$ and $p_{2,c} = 0.55$, and results are discussed in Section 5 with more details.

4.5 Combining the maximum likelihood and quantile methods

As noted in above the quantile method works well for quantiles close to the median of the random variables. Thus the estimates of μ_a and μ_b may be accurate but the estimates of σ_a and σ_b may not due to large approximation errors. As an alternative, we propose a two-step estimation method that combines the quantile method and the maximum likelihood.

First, we estimate μ_a and μ_b from the quantile method using the estimates of the median of T_s and T_c. Second, we estimate σ_a and σ_b by maximizing the likelihood functions using the $\widehat{\mu}_a$ and $\widehat{\mu}_b$ from the first step. This method is more computationally efficient than the likelihood method and it improves the estimates of the standard deviations.

5 Simulation studies

This section simulates the breaking times T_s in the ramp load test and T_c in the constant load test from the US Model, and then apply the parameter estimation methods in the previous section estimate the model parameter $\theta = (\mu_a, \mu_b, \sigma_a, \sigma_b)$. We summarize the results of our simulation study in the final subsection.

5.1 General setup for simulation

We use the same basic plan for all simulation studies reported in this section. We set $\theta = (42, 50, 0.4, 0.4)$ or $\theta = (42, 50, 5, 5)$ and use $p = 0.2$ in the constant load test. We use $n_s = n_c = 200$ in the simulation studies for the three parameter estimation methods proposed in this report. For each simulation run, we generate $n_s = 200$ breaking times the T_s's in the ramp load test and another $n_c = 200$ T_c's in the constant load test from the US Model. This part is the same for all simulation runs. Second, we estimate the parameter θ using the three methods. This part is different for the different parameter estimation methods as seen in the following sections for each parameter estimation method. We repeat the above simulation process $n_{sim} = 100$ times.

5.2 Simulation studies for the approximate MLEs

The approximate likelihood functions are calculated after the approximation steps 1 and 2 for the breaking time T_s in the ramp load test and the breaking time T_c in the constant load test, as discussed in the previous section. To estimate the parameters, we obtain the approximate maximum likelihood estimates numerically from the log-likelihood functions, using the function *nlm* in R. We set the starting point of θ in the optimization process to be the true value of θ. For the optimization process, the maximum iteration step is set to be 20 and the iteration limit is set to be 200. We record the outputs of the optimization results, which indicates why the optimization process terminates. The output of the optimization results is a number from 1 to 5. Codes 1 and 2 mean the optimization converges, Code 3 means the optimization may not converge, and Codes 4 and 5 mean the optimization does not converge.

Results

Figure 5 shows the bar plots of the outputs of the optimization results. Figure 5 shows that, in quite a few simulation runs, the output is not reliable, since many runs lead to code 3 (may not converge). The codes 4 and 5 do not appear in the 100 simulation runs. The approximate maximum likelihood estimates do not work well in this simulation studies. We will explain possible reasons in the next section. Similar results can be shown when $\theta = (42, 50, 5, 5)$. The output of the codes for the approximate maximum likelihood estimates works less well when σ_a and σ_b are large. There we see even more convergence failures.

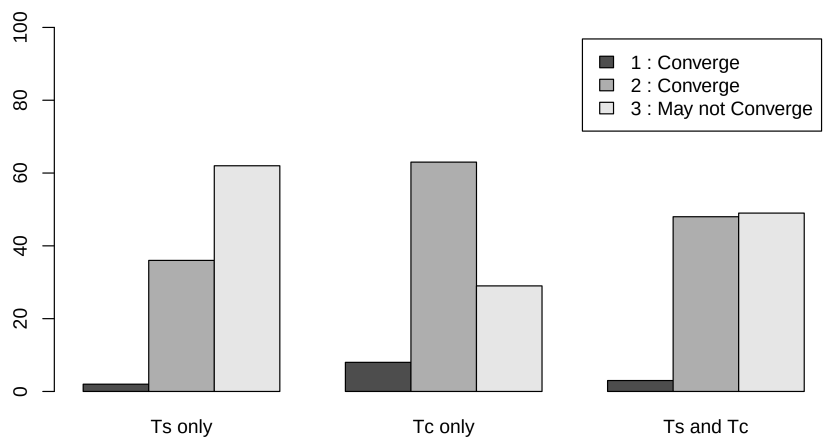

Figure 5: Bar plots of the optimization codes for calculating the approximate maximum likelihoodestimates in $n_{sim} = 100$ simulation runs, when $\theta = (\mu_a, \mu_b, \sigma_a, \sigma_b) = (42, 50, 0.4, 0.4)$, $n_s = n_c = 200$ and $p = 0.2$ in the constant load test.

The likelihood functions

From the results in the previous section, we believe that the reason for the bad performance of the R - program *nlm* may be that the likelihood functions are flat, or even that the approximate maximum likelihood estimate may not be unique. That led us to perform a simulation study to investigate this idea. More precisely, we generate $n_s = 200$ T_s's and $n_c = 200$ T_c's from the US Model when $\theta = (42, 50, 0.4, 0.4)$ and $p = 0.2$ in the constant load test. We calculate the log–likelihood functions for the $\{T_s\}$ in the ramp load test, for the $\{T_c\}$ in the constant load test, and for both the $\{T_s\}$ and $\{T_c\}$, where $\sigma_a = 0.4$ and $\sigma_b = 0.4$ are fixed, while μ_a varies from 40 to 45 and μ_b varies from 47 to 52. The corresponding plots of the log-likelihood functions are shown in Figure 6.

Figure 6 shows that the log-likelihoods do not have an obvious maximum point when σ_a and σ_b are fixed. The log-likelihoods are roughly maximized along the line $\mu_b - \mu_a \approx 8$. As a result, we may not be able to estimate

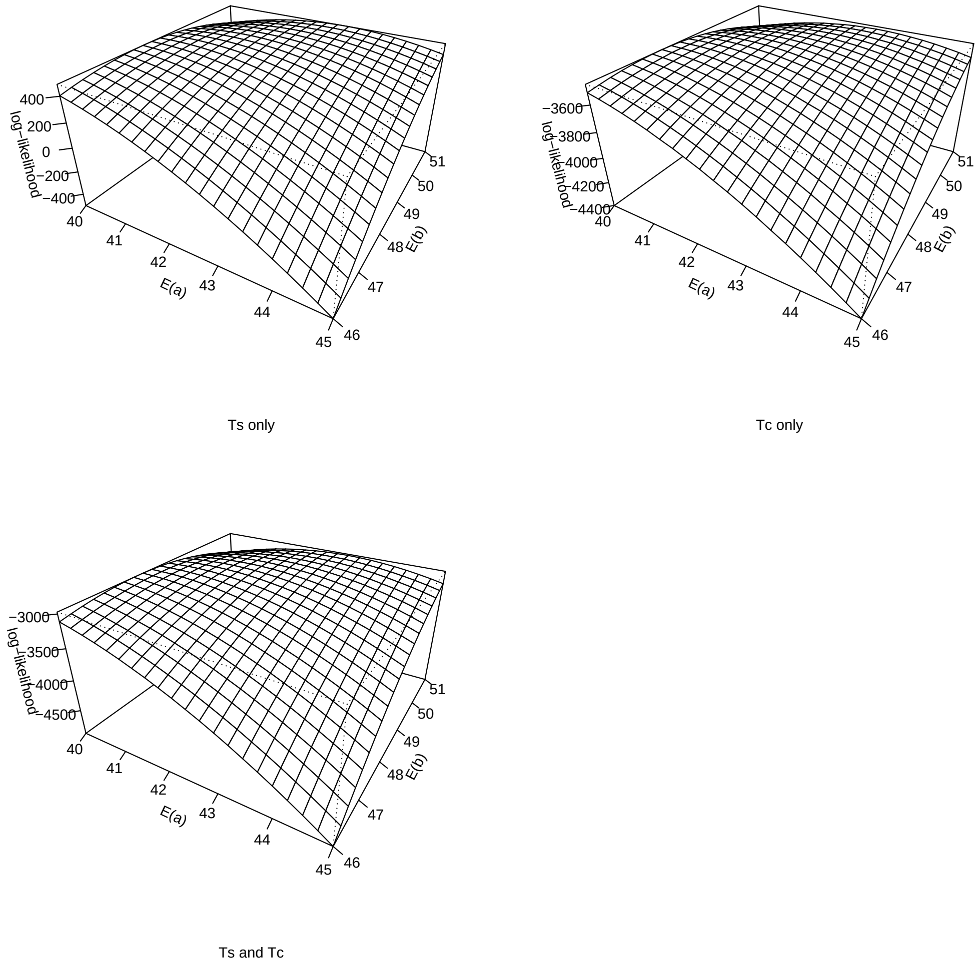

Figure 6: Perspective plots of the log-likelihoods when $\sigma_a = 0.4$ and $\sigma_b = 0.4$ are fixed, and μ_a varies from 40 to 45 and μ_b varies from 47 to 52.

μ_a and μ_b well, but may be able to estimate $\mu_b - \mu_a$. The figure does not prove for the statement that θ can not be estimated using the approximate maximum likelihood estimates from the U.S. model. However, it provides a possible explanation for the bad performance of the approximate maximum likelihood estimates in the previous section.

In conclusion, the approximate maximum likelihood estimates are not reliable for estimating the parameter θ.

5.3 Simulation studies for the quantile method

The simulation setups are the same as that discussed in above except that we also consider the case $n_s = n_c = 200,000$ for illustrative purposes. For $n_s = n_c = 200$, the quantile method estimates μ_a and μ_b well, but it produces negative estimates of σ_a and σ_b in most simulation runs (see (35)). Increasing the sample size to $n_s = n_c = 200,000$ diminishes but does not eliminate the problem. The reason is still unclear at this moment. To illustrate the asymptotic performance of the quantile method for estimating σ_a and σ_b, we use $n_s = n_c = 200,000$ although those numbers are not realistic in practice.

We estimate μ_a and μ_b using the estimates of the medians of T_s and T_c as described above and σ_a and σ_b using the estimates of the quantiles of T_s and T_c. We estimate μ_X and σ_X^2 by the sample mean and sample variance of the T_s's instead of using the median and the quantiles. The results are similar from the two approaches. Here, we only show the simulation results using the median and the quantiles of T_s. The quantiles used in this simulation studies are: $p_{1,s} = 0.2$, $p_{2,s} = 0.8$, $p_{1,c} = 0.45$ and $p_{2,c} = 0.55$.

Results

The simulation results using the quantile method are summarized in Figure 7 and Figure 8. Figure 7 depicts the boxplots for $\widehat{\mu}_a$ and $\widehat{\mu}_b$ for both $n_s = n_c = 200$ and $n_s = n_c = 200,000$, as well as the boxplots for $\widehat{\sigma}_a$ and $\widehat{\sigma}_b$ for $n_s = n_c = 200,000$ only (when $\theta = (42, 50, 0.4, 0.4)$ and $p = 0.2$ in the constant load test). We do not show the boxplots for $\widehat{\sigma}_a$ and $\widehat{\sigma}_b$ when $n_s = n_c = 200$ since the quantile method produces positive estimates for both σ_a^2 and σ_b^2 only in 3 simulation runs out of 100 runs in total.

Figure 8 depicts the boxplots for $\widehat{\mu}_a$, $\widehat{\mu}_b$, $\widehat{\sigma}_a$ and $\widehat{\sigma}_b$ when $n_s = n_c = 200$, $\theta = (42, 50, 5, 5)$ and $p = 0.2$ in the constant load test. Figure 9 depicts the box plots for $\widehat{\mu}_a$, $\widehat{\mu}_b$, $\widehat{\sigma}_a$ and $\widehat{\sigma}_b$ when $n_s = n_c = 200,000$, $\theta = (42, 50, 5, 5)$ and $p = 0.2$ in the constant load test.

From Figure 7, the quantile method estimates μ_a and μ_b well when $n_s = n_c = 200$, and better when $n_s = n_c = 200,000$. The variabilities of the estimates are smaller when n_s and n_c are larger. This can be explained by the fact that, when n_s and n_c are larger, the median estimates for T_s and T_c

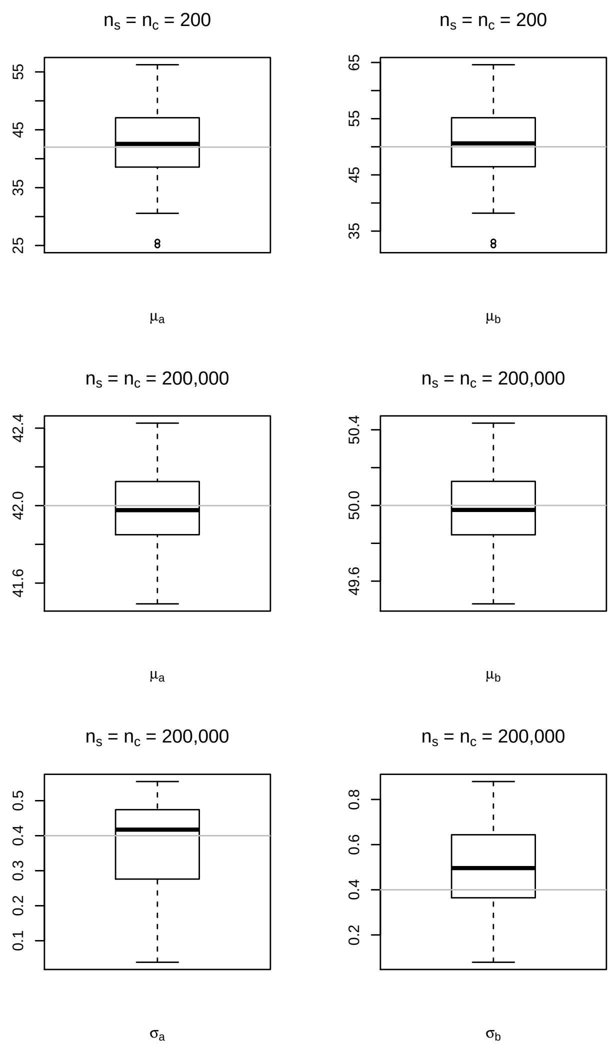

Figure 7: Box lots of the estimates using the quantile method, when $\theta = (42, 50, 0.4, 0.4)$ and $p = 0.2$. The sample size n_s and n_c used in the simulation runs are shown in plot titles. The grey line indicates the true value of the parameter.

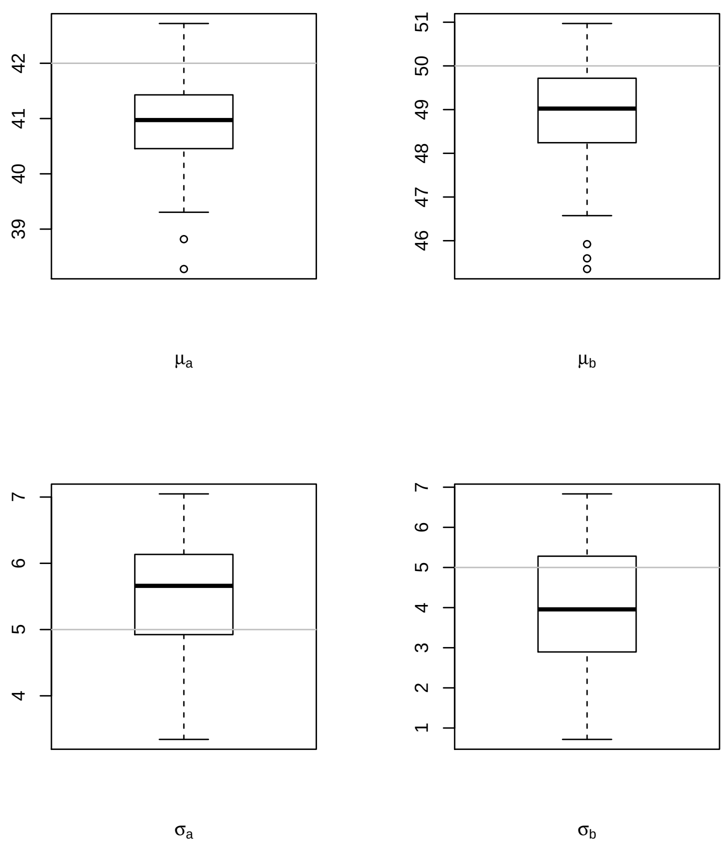

Figure 8: Box lots of the estimates using the quantile method, when $\theta = (\mu_a, \mu_b, \sigma_a, \sigma_b) = (42, 50, 5, 5)$ and $p = 0.2$. The sample size $n_s = n_c = 200$. The grey line indicates the true value of the parameter.

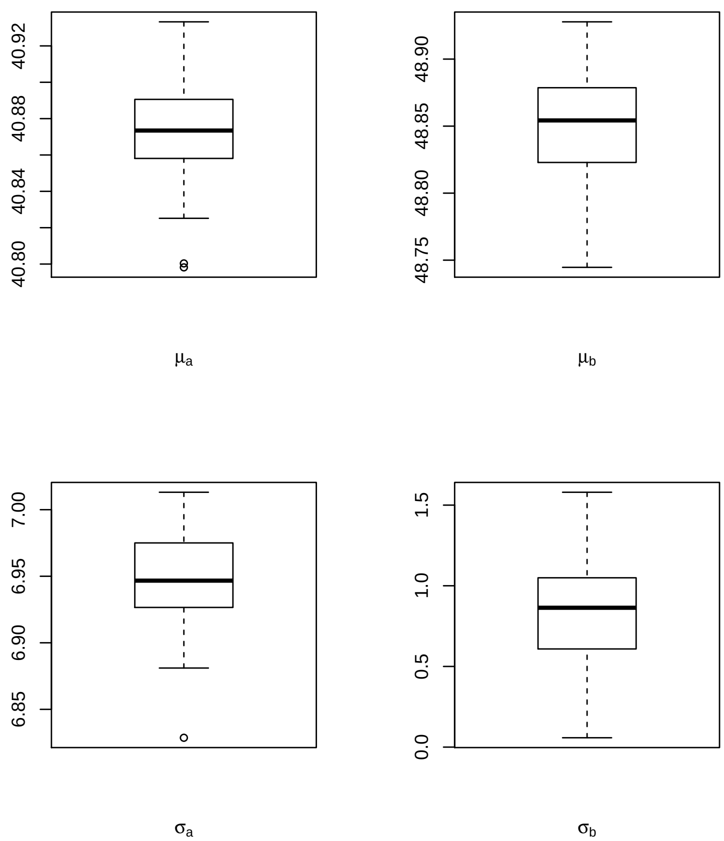

Figure 9: Box lots of the estimates using the quantile method, when $\theta = (\mu_a, \mu_b, \sigma_a, \sigma_b) = (42, 50, 5, 5)$ and $p = 0.2$. The sample size $n_s = n_c = 200,000$. No grey line is shown in the plots because the estimates are too far from the true values.

are more accurate, so the estimates for μ_a and μ_b are more accurate. Similar results can be shown if we use the mean estimate of T_s instead of the median estimate of T_s.

From Figure 7, the quantile method estimates σ_a and σ_b well when $n_s = n_c = 200,000$. The quantile method gives positive estimates for both σ_a^2 and σ_b^2 successfully in 54 simulations runs out of 100 runs, and the box plots show that the estimates are reasonably accurate.

From Figure 8 and Figure 9, the estimates of μ_a and μ_b are biased using the quantile method when $\sigma_a = \sigma_b = 5$. The standard errors of the estimates are smaller when n_s and n_c are larger, but the estimates of μ_a and μ_b are biased in both figures. This can be explained by the fact that, when σ_a and σ_b are large, the approximations 1, 2 and 3 discussed in Section 4.4 are not accurate anymore, as shown in Figure 2 and Figure 3. As a result, although the estimates of the medians of T_s and T_c are accurate when n_s and n_c are large, the equations that link μ_a and μ_b to the median of $\log(T_s)$ and $\log(T_c - T_0)$ do not hold anymore. As a consequence, the estimates for μ_a and μ_b are not accurate.

From Figure 8, the estimates of σ_a and σ_b are still acceptable although the estimates of μ_a and μ_b are not very accurate from the quantile method.

From Figure 9, the estimates of σ_a and σ_b are biased from the quantile method. The quantile method gives positive estimates for both σ_a and σ_b in 57 simulations runs out of 100 runs. This can also be explained by the fact that, when σ_a and σ_b are large, the approximation steps 1, 2 and 3 used for the quantile method are not accurate.

In conclusion, the quantile method estimates μ_a and μ_b well when σ_a and σ_b are small. The quantile method estimates σ_a and σ_b well when σ_a and σ_b are small and the sample sizes are extremely large (e.g., 200,000), or when σ_a and σ_b are large and the sample sizes are small. Note that a sample of size 200,000 is unreasonable in practice. Here we only use it for our critical analysis of the methods.

5.4 Simulation Studies for the combined method

We first estimate μ_a and μ_b using the medians of T_s and T_c, and then estimate σ_a and σ_b by approximate maximum likelihood assuming the true means are $\widehat{\mu}_a$ and $\widehat{\mu}_b$. We can also use the sample mean of T_s instead of the median of T_s. The results are similar for the two approaches. Here, we only show the simulation outputs resulting from use of the median of T_s. To calculate the approximate maximum likelihood estimates of σ_a and σ_b, we use the approximate likelihood functions after the approximation steps 1 and 2 for both T_s's and T_c's given $\widehat{\mu}_a$ and $\widehat{\mu}_b$ from the quantile estimates. We choose the starting point (σ_a, σ_b) for the optimization process to be the true value, and random values uniformly generated from an area contains the true value for each simulation run. The area is $0 < a < 1$ and $0 < b < 1$ for $(\sigma_a, \sigma_b) = (0.4, 0.4)$, and $0 < a < 10$ and $0 < b < 10$ for $(\sigma_a, \sigma_b) = (5, 5)$.

Results

The simulation results are summarized in Figure 10 to Figure 12. Figure 10

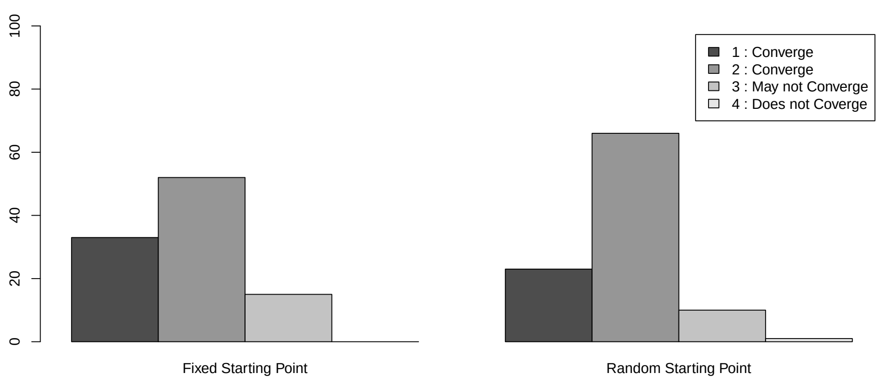

Figure 10: Bar plots of the output of the optimization results in calculating the approximate maximum likelihood estimates for σ_a and σ_b in the combined method when $\theta = (\mu_a, \mu_b, \sigma_a, \sigma_b) = (42, 50, 0.4, 0.4)$ and $p = 0.2$ in the constant load test. Fixed starting point means the starting point in the optimization step of the combined method is set to be the true value $(\sigma_a, \sigma_b) = (0.4, 0.4)$. Random starting point means the starting point in the optimization step of the combined method is set to be different random numbers uniformly generated from the square $0 < \sigma_a < 1$ and $0 < \sigma_b < 1$ for different simulation runs.

contains the bar plots of the outputs of the optimization results for maximizing the approximate likelihood using the combined method when $\theta =$

$(42, 50, 0.4, 0.4)$ and $p = 0.2$ in the constant load test. Comparing Figure 10 to Figure 5, we notice that the optimization process converges in the combined method for most simulation runs, better than the optimization process in the approximate maximum likelihood method. This means that we are able to estimate σ_a and σ_b for most simulation runs given $\widehat{\mu}_a$ and $\widehat{\mu}_b$ from the quantile estimates.

Figure 11 contains the plots for the estimates of σ_a and σ_b from the combined method when $\theta = (42, 50, 0.4, 0.4)$. In Figure 11, the starting point for the optimization process in the second step is chosen to be the true value $(\sigma_a, \sigma_b) = (0.4, 0, 4)$, as well as random starting numbers generated uniformly from the square $0 < \sigma_a < 1$ and $0 < \sigma_b < 1$. The box plots for $\widehat{\mu}_a$ and $\widehat{\mu}_b$ are shown in Figure 7.

Figure 12 contains the plots for the estimates of σ_a and σ_b from the combined method when $\theta = (42, 50, 5, 5)$. In Figure 12, the starting point for the optimization process in the second step is chosen to be the true value $(\sigma_a, \sigma_b) = (5, 5)$, as well as random starting numbers generated uniformly from the square $0 < \sigma_a < 10$ and $0 < \sigma_b < 10$. The box plots for $\widehat{\mu}_a$ and $\widehat{\mu}_b$ have been shown in Figure 8.

From Figure 11, the combined method estimates σ_a and σ_b well in both the fixed starting point condition and the random starting point condition. The estimates are less variable when the starting point is chosen to be the true value. From the two middle panels of Figure 11, the combined method still works acceptably well when the starting points are random numbers. However, from the two lower panels of Figure 11, the estimates of σ_a and σ_b are not the same as those when the starting points are chosen to be the true value for some simulation runs. The starting points influence the estimates for some simulation runs, but do not influence the centre of the overall distributions of the estimates much.

From Figure 12, the combined method estimates σ_a and σ_b acceptably well in both the fixed starting point condition and the random starting point condition, although the estimate of σ_b is slightly biased. Combined with Figure 8, Figure 12 shows that, although the combined method does not estimate μ_a and μ_b well in the first step, it still estimates σ_a and σ_b acceptably well using the estimates of μ_a and μ_b from the first step. From the two lower panels of Figure 12, the combined method is not sensitive to the choice of the starting point in the optimization when $\sigma_a = \sigma_b = 5$.

In conclusion, the combined method estimates the parameters θ well when σ_a and σ_b are small. The combined method estimate the parameter σ_a and

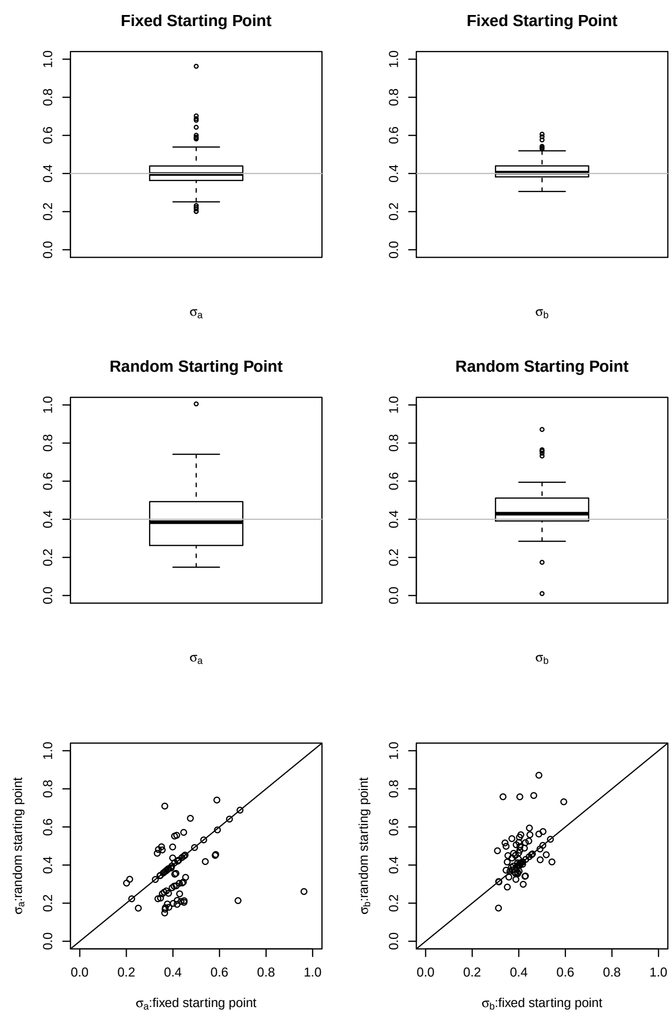

Figure 11: Plots of the estimates for σ_a and σ_b when $\theta = (42, 50, 0.4, 0.4)$ and $p = 0.2$ in the constant load test. Fixed starting point means the starting point in the optimization step of the combined method is set to be the true value $(\sigma_a, \sigma_b) = (0.4, 0.4)$. Random starting point means the starting point in the optimization step of the combined method is set to be different random numbers in the square $0 < \sigma_a < 1$ and $0 < \sigma_b < 1$ for different simulation runs. The grey line indicates the true value of the parameter.

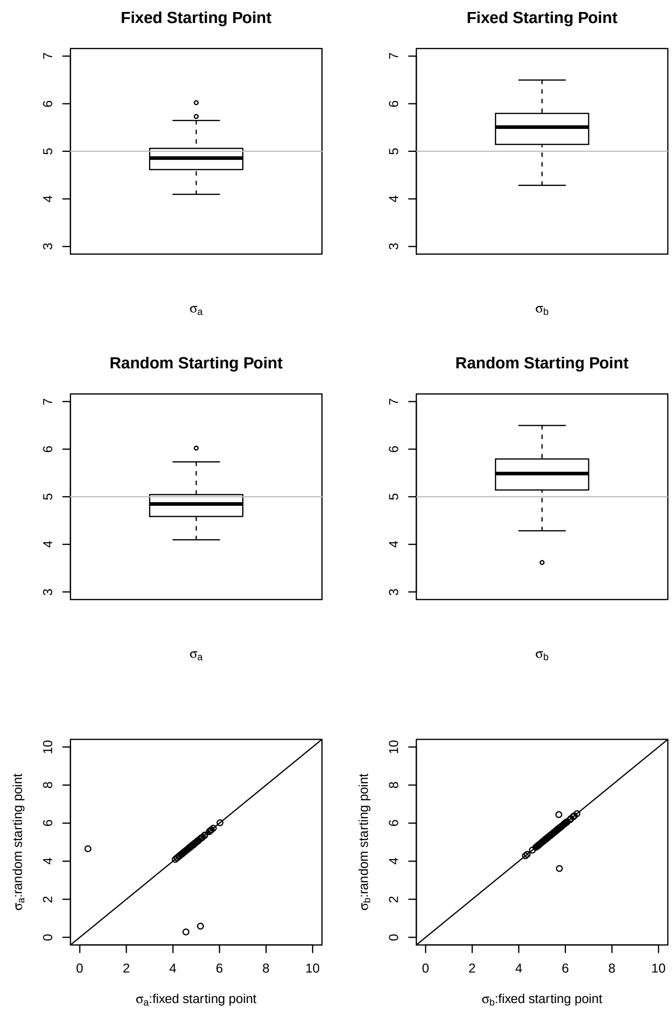

Figure 12: Plots of the estimates for σ_a and σ_b when $\theta = (42, 50, 5, 5)$ and $p = 0.2$ in the constant load test. Fixed starting point means the starting point in the optimization step of the combined method is set to be the true value $(\sigma_a, \sigma_b) = (5, 5)$. Random starting point means the starting point in the optimization step of the combined method is set to be different random numbers in the square $0 < \sigma_a < 10$ and $0 < \sigma_b < 10$ for different simulation runs. The grey line indicates the true value of the parameter.

σ_b well even if $\widehat{\mu}_a$ and $\widehat{\mu}_b$ from the first step of the combined method are not very accurate. The combined method is not very sensitive to the choice of the starting point for optimization in the second step.

5.5 Summary of the simulation results

Table 1 summarizes main simulation results in this section. The lessons learned are stated in Section 7.

Methods (σ_a, σ_b)	$mean(\widehat{\mu}_a) - \mu_a$ (s.e.)	$mean(\widehat{\mu}_b) - \mu_b$ (s.e.)	$mean(\widehat{\sigma}_a) - \sigma_a$ (s.e.)	$mean(\widehat{\sigma}_b) - \sigma_b$ (s.e.)	Success Rates
Approx MLE (0.4, 0.4)	-	-	-	-	0.51
Quantile (0.4, 0.4)	0.736 (0.652)	0.740 (0.670)	-0.125 (0.028)	0.058 (0.028)	0.03 (1 for $\widehat{\mu}_a$ and $\widehat{\mu}_b$)
Quantile (5, 5)	-1.065 (0.078)	-1.101 (0.116)	0.539 (0.131)	-0.913 (0.192)	0.54 (1 for $\widehat{\mu}_a$ and $\widehat{\mu}_b$)
Combined (0.4, 0.4)	0.736 (0.652)	0.740 (0.670)	0.014 (0.010)	0.016 (0.006)	0.85 (fixed start)
	0.736 (0.652)	0.740 (0.670)	0.256 (0.012)	0.450 (0.006)	0.89 (random start)
Combined (5, 5)	-1.065 (0.078)	-1.101 (0.116)	-0.192 (0.059)	0.492 (0.048)	0.95 (fixed start)
	-1.065 (0.078)	-1.101 (0.116)	-0.245 (0.076)	0.476 (0.053)	0.93 (random start)

Table 1: Summary of the simulation results in Section 5 when $n_s = n_c = 200$. In all simulation runs, $(\mu_a, \mu_b) = (42, 50)$ and in the constant load test $p = 0.2$. The values of (σ_a, σ_b) are shown in the table. The success rates denote the proportion of the converged simulation runs for the approximate maximum likelihood estimates and the combined method, and the rates of the simulation runs which produce positive estimates for both σ_a^2 and σ_b^2 for the quantile method.

6 Experiment and data analysis

This section demonstrates use of our parameter estimation methods on the pioneering experiments of Foschi and Barrett (1982), who investigated the duration of load effects and analyze the breaking times T_c's from their constant load tests, where the load level is set to be the 20-th percentile of the short term strength. The data were analyzed by a modification of the combined method we proposed in Section 4.5.

6.1 Foschi and Barrett's Experiments

In the 1980s, Foschi and Barrett (1982) conducted an experiment to assess the duration of load effects on western hemlock lumber of size 2 inches by 6 inches, and grade No. 2 and better. They conducted a ramp load test with a sample size of 150, and then conducted two constant load tests: one with the load level set to be the 20-th percentile and the other with load level set to be the 5-th percentile of the short-term strength. The initial sample size for each constant load test was 500. However, some wood specimens were discontinued after three months for unreported reasons. So the final sample sizes in the one year experiment are 400 wood specimens for the 20-th percentile constant load group and 300 wood specimens for the 5-th percentile constant load group. More details about Foschi and Barrett's experiments can be found in Foschi and Barrett (1982).

In the constant load test of the Foschi – Barrett experiment when $p = 0.2$, 207 wood specimens out of 400 broke within one year. Foschi and Barrett did not report how many of them broke during the ramp loading part of the constant load tests nor did they specify the value of T_0. However, they wrote that 20% of the wood specimens in this test failed during the ramp loading part, as expected. Since the 79-th, 80-th, 81-st and 82-nd order statistics of the breaking times T_c's are the same in this dataset, we assume that 82 wood specimens broke during the ramp loading part of the constant load test in our analysis, and assume the 82–nd order statistic of the breaking times T_c's to be T_0.

6.2 Data analysis

This section presents the results of an analysis of the breaking times T_c's from the Foschi – Barrett experiments when the load level is set as the 20^{th} percentile of the short term strength. We did not use the approximate maximum likelihood estimates to estimate parameters for this dataset since the approximate maximum likelihood estimates may well be unreliable according to the results of our simulation studies. Nor could we apply the quantile methods and the combined method proposed in Section 4 directly to this dataset since we do not have the ramp load test results from their experiments. Thus we improvised and used a revised method that combines the approximate maximum likelihood and quantile methods for the breaking times T_c's only. The only difference between the revised combined method here and the combined method in Section 4.5 is the novel way we used to estimate μ_X.

Recall that the breaking time T_c can be written as

$$T_c = \begin{cases} X, & \text{if } X \leq T_0, \\ Y, & \text{if } X > T_0, \end{cases} \tag{48}$$

where

$$X = \frac{\exp(a)b}{\exp(b) - 1}, \tag{49}$$

and

$$Y = T_0 + \frac{\exp(a)}{\exp(b) - 1}\left[\exp\left\{b - T_0\frac{\exp(b) - 1}{\exp(a)}\right\} - 1\right]. \tag{50}$$

In the first step of the combined method in Section 4.5, we estimate μ_a and μ_b from μ_X and μ_Y, as in (32). We estimate μ_X by the median of $\log(T_s)$, and estimate μ_Y by the median of $\log(T_c - T_0)$. In the second step of the combined method, we estimate σ_a and σ_b by the approximate maximum likelihood using $\widehat{\mu}_a$ and $\widehat{\mu}_b$ from the first step.

For this dataset, to estimate μ_Y, we can still use the median of $\log(T_c - T_0)$ as discussed in Section 4.5. To estimate μ_X, we cannot use the median of $\log(T_s)$ since we do not have those T_s's. However by definition, those T_c's, which are less than T_0, equal X. Thus we fit the first 82 order statistics of the logarithm of the breaking times T_c's to a truncated normal distribution using the function *survreg* in R, and estimate μ_X by the mean of that normal distribution.

After we estimated μ_a and μ_b from $\widehat{\mu}_X$ and $\widehat{\mu}_Y$, we estimated σ_a and σ_b by maximizing the approximate likelihood function for T_c's as discussed in Section 4.5, using $\widehat{\mu}_a$ and $\widehat{\mu}_b$ from the first step. These steps are all the same as the combined method in Section 4.5 .

For the optimization process in the second step discussed in Section 4.5, we choose the starting points for σ_a and σ_b randomly from the uniform distribution in $(0, 1)$. We repeated the optimization process 100 times with different starting points. The results of the optimization show that 89 runs out of 100 runs converge. We estimated σ_a and σ_b by the medians of the 89 estimates of σ_a and σ_b in these 100 runs. The boxplots of the 89 estimates of σ_a and σ_b are shown in Figure 13.

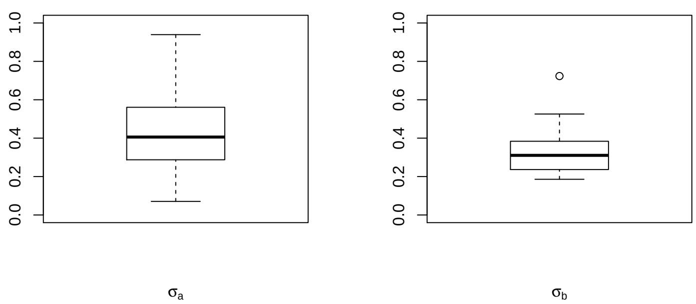

Figure 13: Box plots of the 89 estimates of σ_a and σ_b.

The resulting estimates are $\widehat{\mu}_a = 41.6997$, $\widehat{\mu}_b = 49.6804$, $\widehat{\sigma}_a = 0.4057$ and $\widehat{\sigma}_b = 0.3105$. These estimates of μ_a and μ_b are close to Gerhards and Link's estimates of a and b ($\widehat{a} = 43.17$ and $\widehat{b} = 49.75$) when a and b are considered as fixed in their approach.

7 Conclusions

This report has presented three methods for estimating the parameters of the US Model for describing the duration of load effect on the strength of wood specimens. We have shown how they may be implemented using certain judicious approximations of the time to failure in standard duration of load tests and standard R codes. The goal of the research reported here was an alternative based on methods in contemporary statistical science to others that had been proposed over the years.

The complexity of the models rules out analytical assessment and hence an extensive simulation study was carried out of the methods. Our findings on the three methods evaluated in this paper are summarized below.

Approximate maximum likelihood. The approximate maximum likelihood estimates described in the report are not reliable since the optimization process in this method only converges in 51 runs out of 100 runs when the likelihood function for both T_s's and T_c's are used. We do not report the estimates of the parameters because the estimates do not make sense when only half of the results from the simulation runs are reliable.

Quantile method. The quantile method estimates μ_a and μ_b well but fails to estimate σ_a and σ_b in most simulation runs. It produces reasonable estimates for μ_a and μ_b in all simulation runs, but only produces positive estimates for σ_a^2 and σ_b^2 in 3 runs out of 100 runs when $\sigma_a = \sigma_b = 0.4$, and only produces positive estimates for σ_a^2 and σ_b^2 in 54 runs out of 100 runs when $\sigma_a = \sigma_b = 5$.

Combined method. The combined method works well in estimating μ_a, μ_b, σ_a and σ_b. In Table 1, the fixed start means the starting points are chosen to be the true values of the parameters, and the random start means the starting points are chosen to be random numbers. The mean of the estimates in the successful runs are shown in Table 1. The medians of the estimates in the successful runs, which are shown in the box plots in the previous sections, are generally closer to the true values than the means of the estimates for most simulation studies.

The report also demonstrates use of our inferential procedures on data collected in a pioneering experiment reported by Foschi and Barrett (1982). Reassuringly, the results obtained closely resembled others that had been reported earlier in the literature.

The importance of the work reported in this papers lies in the application to innovative manufactured wood products that are now coming on stream for structural engineering applications. We believe the work has laid a statistical foundation for incorporating the results of testing in establishing design values for those products.

References

[1] American Society for Testing and Materials (ASTM). ASTM D 6815 09. Standard Specification for Evaluation of Duration pf Load and Creep Effects of Wood and Wood-Based Products. ASTM International, 100 Barr Harbor Drive, PO Box C700, West Conshohocken, PA 19428-2959, United States.

[2] Barrett, J. D. and Foschi, R. O. (1978). Duration of load and probability of failure in wood. Part I: modelling creep rupture. *Canadian Journal of Civil Engeneering*, Vol. 5, No. 4: 505-514.

[3] Barrett, J. D. and Foschi, R. O. (1978). Duration of load and probability of failure in wood. Part II: constant, ramp and cyclic loadings. *Canadian Journal of Civil Engeneering*, Vol. 5, No. 4: 515-532.

[4] Cai, Z., Rosowsky, D. V., Hunt, M. O. and Fridley, K. J.(2000). Comparison of actual vs. simulated failure distributions of flexural wood specimens subject to 5-day load sequences. *Forest Products Journal*, 50(1): 7480.

[5] Foschi, R. O. and Barrett, J. D. (1982). Load-duration effects in western hemlock lumber. *ASCE Journal of the Structural Division*, Vol. 108(7): 1494-1510.

[6] Foschi, R. O. and Yao, F. Z. (1986). Another look at three duration of load models. *In Proceedings of IUFRO Wood Engineering Group Meeting*, Florence, Italy, paper: 19-9-1,

[7] Gerhards, C. C. (1977). Effects of duration and rate of loading on strength of wood and wood-based materials. *Madison: USDA Forest Services Research Report*, FPL 283

[8] Gerhards, C. C. (1979). Time-related effects of loading on wood strength: a linear cumulative damage theory. *Wood Science*, 11(3): 139-144.

[9] Gerhards, C. C. and Link, C. L. (1987). A cumulative damage model to predict load duration characteristics of lumber. *Wood and Fiber Science*, 19(2): 147-164, 1987.

[10] Hendrickson, E. M., Ellingwood, B. and Murphy, J. Limit state probabilities for wood structural members. *Journal of Structural Engineering*, 113, 88–106.

[11] Karacabeyli, E. and Soltis, L.A. (1991). State of the art report on duration of load research for lumber in North America. Proceedings of the 1991 International Timber Engineering Conference. London, United Kingdom.

[12] Markwardt, L.J. and Liska, J.A. (1948). Speed of Testing of Wood. Factors in its Control and its Effect on Strength. *Proc. ASTM*, 48:1139-115.

[13] Wang, J. B. (2009). Duration-of-load and creep behavior of thick MPB strand based wood composite. Ph.D. thesis. Faculty of Forestry, the University of British Columbia.

[14] Wood, L. W. (1951). Relation of strength of wood to duration of load. *Madison: USDA Forest Service Report*, No. 1916.

[15] Yao, F. Z. (1987). Reliability of structures with load history-dependent strength of an application to wood members. Master thesis. Department of Civil Engineering, the University of British Columbia.

[16] Zhai, Y. (2012) Duration of Load models. MSc Thesis, Department of Statistics, University of British Columbia.

[17] Zhai, Y., Pirvu, C., Heckman, N., Lum, C., Wu, L. and Zidek, J.V. (2012). A review of dynamic duration of load models for lumber strength. TR 270, Department of Statistics, University of British Columbia.